SOLUTE TRANSPORT THROUGH LABORATORY-SCALE KARSTIC AQUIFERS

LEE J. FLOREA
Kentucky Cabinet for Natural Resources, Dept. of Surface Mining Reclamation and Enforcement, Office of the Commissioner, #2 Hudson Hollow, Frankfort, KY 40601, lee.florea@mail.state.ky.us
CAROL M. WICKS
Department of Geological Sciences, University of Missouri – Columbia, Columbia MO 65211, wicksc@missouri.edu

Laboratory-scale models of branchwork and of network karstic aquifers were constructed to provide data needed for calibration of numerical models. The distribution and connectedness of the conduits and sinkholes were scaled similarly to those found in nature; however, the porosity of models (2 and 3%) and the recharge rate (80 cm/hr) could not be scaled appropriately. Pulses of 1-M NaCl were injected sequentially at ten locations on both models to determine transport parameters using QTRACER. For all experiments, the Reynolds numbers were <150, the Peclet numbers were >6, and the Froude numbers were ~0. The flow regime was laminar and subcritical and advective processes dominated transport processes. The mean tracer transit times were significantly greater in the network model (29 s and 49 s) than in the branchwork model (17 s and 35 s) for injection locations that were proximal to (<10 cm) and distal from (10-20 cm) the spring. The lag times and times to peak concentration were highly variable and no systematic variation with distance from the spring could be discerned. The results can be used in calibration of numerical models of tracer transport through karstic aquifers.

Numerical models have been developed to predict how groundwater flow and tracer transport occurs through karstic aquifers (Teutsch 1994; Mohrlok & Teutsch 1997; Mohrlok & Sauter 1997; Mohrlok *et al.* 1997; Annabelle & Sudicky 1999; Quinn & Tomasko 2000; Peterson & Wicks 2000). One important step in evaluating numerical models is model calibration in which the results from a modeling effort are compared to results from field or laboratory studies (Anderson & Woessner 1992). The calibration of numerical models has been hindered by a lack of data from field and laboratory experiments in which the flow paths are known. Thus, the goal of this study was to provide data that are needed for calibration of numerical models by conducting well-controlled tracer transport experiments in constructed laboratory-scale models of karstic aquifers.

Palmer (1999) clearly states the pitfalls of building scale models and interpreting the results from scale models. The laboratory model must reflect more than a reduction of the scale of physical parameters (length, conduit size, etc.) and it must maintain similar forces. Palmer (1999) suggests that critical parameters are the Reynolds number and Froude number for modeling flow through open and closed channels. As the experiments conducted in this study are solute transport experiments, the Peclet number is also critical as it compares movement of the solute by advection to that due to diffusion.

Several other studies have relied on construction of laboratory-scale models of aquifers to gain a better understanding of flow and transport processes. Silliman *et al.* (1987), Saiers & Hornberger (1994), and Saiers *et al.* (1994) used small-scale models of modified sand-packed columns to study contaminant transport through porous media. Toran & Palumbo (1992) and Ibaraki & Sudicky (1995a; 1995b) used small-scale models of fractured media to study colloidal transport and solute transport. The main use of small-scale models of karstic aquifers has been for studies related to the formation of dissolutional features (Ewers 1972; Glew 1977). Recently, Jeannin *et al.* (1999) developed a small-scale model of one reach of cave stream to study dispersion. Our objectives were to develop laboratory-scale models of karstic aquifers, to conduct tracer transport experiments, to clearly document problems encountered, and therefore to provide data that can be used in calibrating numerical models.

CONSTRUCTION OF THE MODELS

Based on measurements on over five hundred cave maps, Palmer (1991) has described five conduit patterns. He found that branchwork conduits represent 57% of the total conduit length and network conduits represent 17% of the total conduit length. The other three types are anastomotic (3%), ramiform (9%), and single conduit (1%) (Palmer 1991). Because hydrogeologic conditions consistent with branchwork and network patterns are predominant in nature, we have chosen to build a model of branchwork and a model of network conduit systems. Both models were created using the same construction method and materials.

Table 1. Porosity and permeability of the cores of fired ceramic clay.

Material	Temperature (°C)	Porosity (%)	Permeability (μDarcys)
Hawthorn 35 mesh	970	4±0.15	33.5±14.5
	1100	10±0.20	12.6±0.01
	1300	2±0.15	6.4±51.7
20-mesh fireclay	970	12±0.06	154±51.7
	1100	8±0.06	177±25.5
	1300	2±0.06	25.2±0.01
Red Earthenware	970	13±0.81	637±85
	1100	3±0.10	25.2±0.01
	1300	NA[1]	NA[1]

[1] The samples of red earthenware that were fired at 1300°C flowed (fluxed).

CONSTRUCTION MATERIALS

Because our objective was to document flow characteristics and not dissolution processes, the choice for the modeling material was based on the needs that the material must be easily molded and acquire characteristics of karstic limestones (low matrix permeability and porosity and high secondary permeability). Two choices were plaster of Paris and ceramic clays. Because plaster of Paris dissolves in water, ceramic clays were chosen. Three ceramic clays were available for use: Hawthorn 35 mesh, 20 mesh fireclay, and red earthenware clay. The kiln could be set to three temperatures 970°C, 1100°C, and 1300°C. Three cores (3.8-cm in diameter and 1.0-cm in height) of each material for each temperature were made and fired. After firing and cooling, the porosity and permeability of each core were determined by calculating the change in weight by saturation with water and by using a falling-head permeameter. From these test results (Table 1), the 20-mesh fireclay fired at 970°C was found to provide the best match to the porosity (12%) and permeability (154 μdarcys) for the Burlington Formation of the mid-continent (Hoag 1957). We chose to represent the Burlington Formation because of its widespread distribution throughout the mid-continent and because of its ecological importance to Ozark cavefish (Bergstrom 1997).

FORMING THE MODELS

Using a process similar to lost-wax casting, a 10 cm x 10 cm x 5 cm frame of plywood was constructed for use in making the models (Fig. 1). Into the frame, moist ceramic clay was pressed to a depth of 3 cm. The pattern for the conduits was laid in place using strands of yarn. The yarn was chosen because it was thick enough to support the weight of the wet clay and because it would completely burn when the model was fired in the kiln. This process left conduits where the yarn had been. A 2-cm thick top portion of the moist ceramic clay was gently laid on top of the strands of yarn and lower layer of clay (the base of the model). The seam between the top portion and the base was sealed using finger pressure. Into the top surface of the top of the model were carved sinkholes (described below) and an epikarstic surface (also described below). The completed ceramic models were air dried for several days and then were fired at 970°C, which completely burned the yarn and left conduits. After the models had cooled, all of the outer surfaces, except for the top of the models, were coated with melted wax, which once hardened served as no-flow boundaries. A detailed description of the construction process is available in Florea (1998).

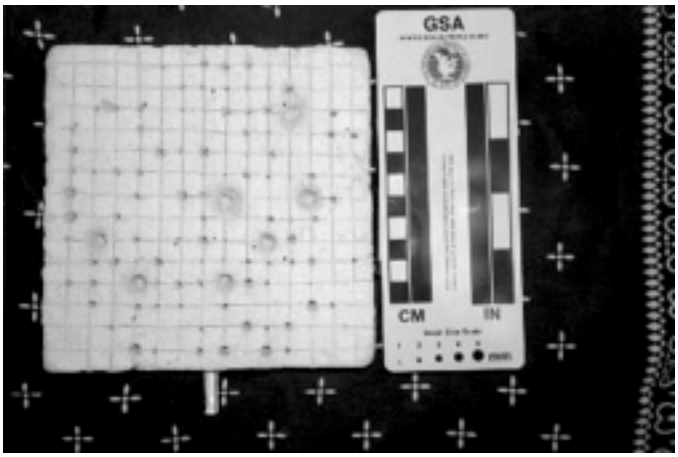

Figure 1. Photograph looking down onto the top of the branchwork model, the sinkholes are visible as is the epikarstic surface (grid pattern).

SINKHOLES

Karstic aquifers receive recharge via diffuse flow (slow percolation) through the matrix, relatively rapid recharge through fractures, and more rapid flow through sinkholes and losing streams (White *et al.* 1995). Therefore, the models had to include locations for rapid recharge (sinkholes). The location and diameter of each sinkhole had to be specified. The possible locations for sinkholes were specified by creating a Cartesian grid with 1-cm on center spacing on the surface of the models (Fig. 2). The grid intersections represented all possible sinkhole locations. Representative diameters of six classes of sinkholes were calculated from the depth-distribution function using the coefficient for Missouri karst (Troester *et al.* 1984). The class with the largest diameter sinkholes had the lowest frequency of occurrence. The location of each and every sinkhole was determined by drawing random numbers representing grid locations on the surface of the model. The number of sinkholes of a given class and the distribution of the sinkholes on the surface of the models were the same between the two models (Fig. 2).

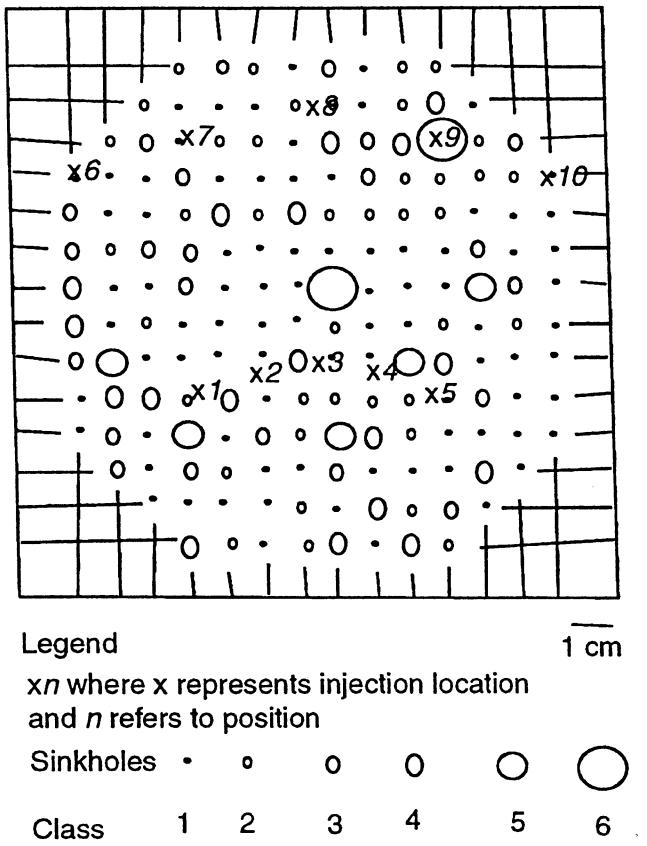

Figure 2. Diagram of a partial grid pattern representing the epikarstic surface, of the injection locations, and of the location and diameter of all sinkholes.

CONDUITS

The number and diameter of the conduits were calculated using the work of Curl (1986), who showed that the number of conduits of a given diameter can be calculated if the fractal dimension is known. In this study, the fractal dimension used was 2.5 (Curl 1986). A conduit segment connects two adjacent grid locations and had a 1-cm length. The diameter of any given segment was calculated using fractal statistics. The resulting distribution of diameters was grouped into five classes. The locations of the segments of a given class were determined by using the distribution of sinkholes on the surface of the models (larger conduits are needed to carry the extra recharge provided by larger sinkholes). In addition, the diameter of the conduits increased in the direction of groundwater flow (Padilla & Pulido-Bosch 1995). Both models were created with the same number of conduit segments of a given class.

The difference between the two models was the conduit morphology (branchwork or network). Branchwork morphologies are dendritic in the distribution of conduits and have only one path from any input location to the spring (Fig. 3a). Network morphologies (mazelike) contain conduits that are highly interconnected. Within network systems, multiple paths exist from any input point to the spring (Fig. 3b). It is noted

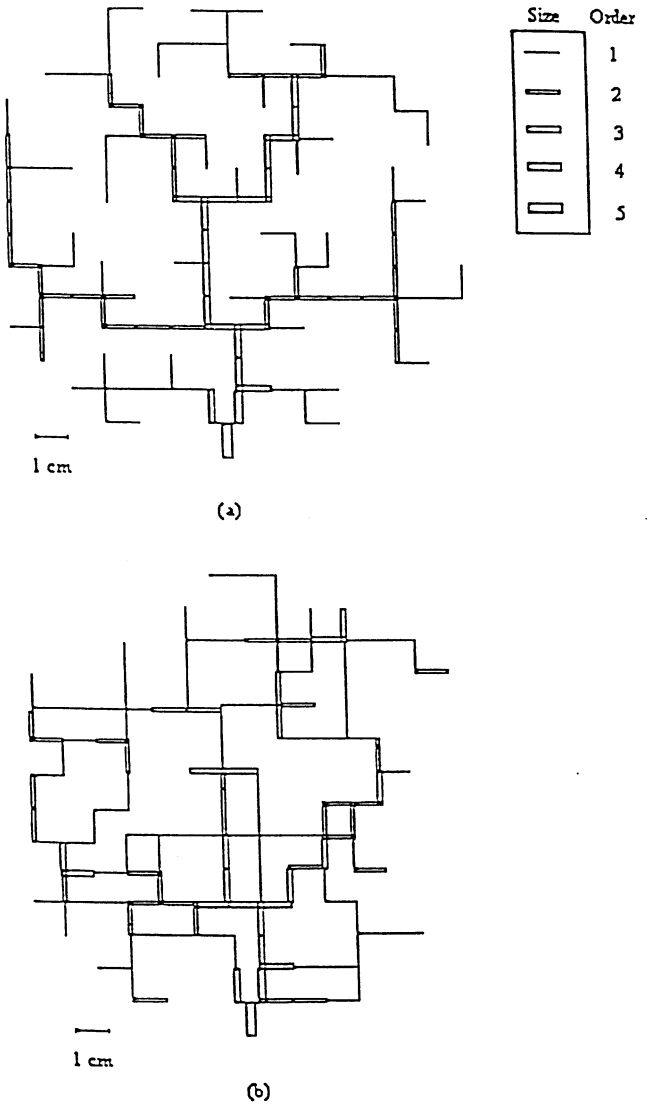

Figure 3. Diagram of the patterns of conduits in the a) branchwork model; b) network model. The sinkholes penetrate vertically downward into the horizontal plane along which the conduits are developed.

that the geometries created within the models are a subset of all possible geometries for each of the morphologies. It is also noted that karst aquifers can exhibit a combination of morphologies (Palmer 1991) that were not considered in this study.

The conduits were made from a worsted 4-ply yarn, chosen because the material burns when fired at 970°C and leaves only an ash residue. One strand of yarn was used to represent a first-class conduit segment with a diameter of 0.10 cm. Two strands of yarn loosely twisted together formed the second-class conduit with a diameter of 0.20 cm (three strands: third-class conduit with diameter 0.30 cm; four strands: fourth-class conduit with diameter 0.40 cm; five strands: fifth-class conduit with diameter 0.50 cm). The yarn was laid upon a foundation of ceramic clay in the required pattern and then the upper part of

Table 2. Average results from the tracer transport experiments using the branchwork model. Each result is the average of three independent experiments.

Model	Lag (s)	Peak (s)	Mean (s)	DL (cm)	Pathlength (cm)	Pe	Re	Fr	Delta (mm)	N	Recovery (%)
location 1	1	14	21	1.3	10	14.0	108.0	0.014	0.14	3	33
location 2	2	11	12	0.8	8	14.0	117.3	0.016	0.11	3	31
location 3	3	11	22	3.5	7	6.3	98.0	0.011	0.15	3	40
location 4	3	10	20	1.8	8	8.7	97.3	0.012	0.14	3	28
location 5	2	12	12	1.0	8	8.3	119.0	0.016	0.11	3	30
location 6	5	15	37	6.2	18	10.7	109.7	0.014	0.17	3	26
location 7	4	16	36	3.6	16	17.0	103.0	0.011	0.17	3	20
location 8	7	18	34	2.7	19	14.3	115.7	0.016	0.15	3	20
location 9	4	17	22	1.2	17	22.0	123.7	0.017	0.14	3	35
location 10	3	15	44	17.0	21	8.0	110.3	0.015	0.18	3	28

the model that incorporated the sinkholes was gently laid on top.

THE EXPERIMENTS AND DATA ANALYSES

CHARACTERIZATION OF THE FLOWPATHS

Because the internal geometry of the models was controlled during construction, the length of each flowpath was known. The lengths in the branchwork model were similar to the shortest paths in the network model (Fig. 4; Tables 2 & 3). Because the number and diameter of all conduit segments along each and every path were known, the theoretical pore volumes of the entire model (9.89 mL for both models) and of each and every path (Fig. 4) were calculated. The actual pore volume of each model was measured by completely saturating the lower portion of the model with water, plugging the spring, and carefully measuring the amount of water needed to completely fill the conduits to the bottom of the sinkholes. Though the pore volumes for the two models should be equal as they contain the same number of conduit segment of the same diameter, the measured pore volume of the network model (12.8 mL ±0.29 mL) was significantly greater than that of the branchwork model (10.2 mL ±0.29 mL). Significantly more secondary porosity was created in the network model than in the branchwork model during the firing process. It is conceivable that the interconnectedness of the conduits within the network model allowed separation along a plane of weakness (between the upper and lower portions of the models) during the firing process.

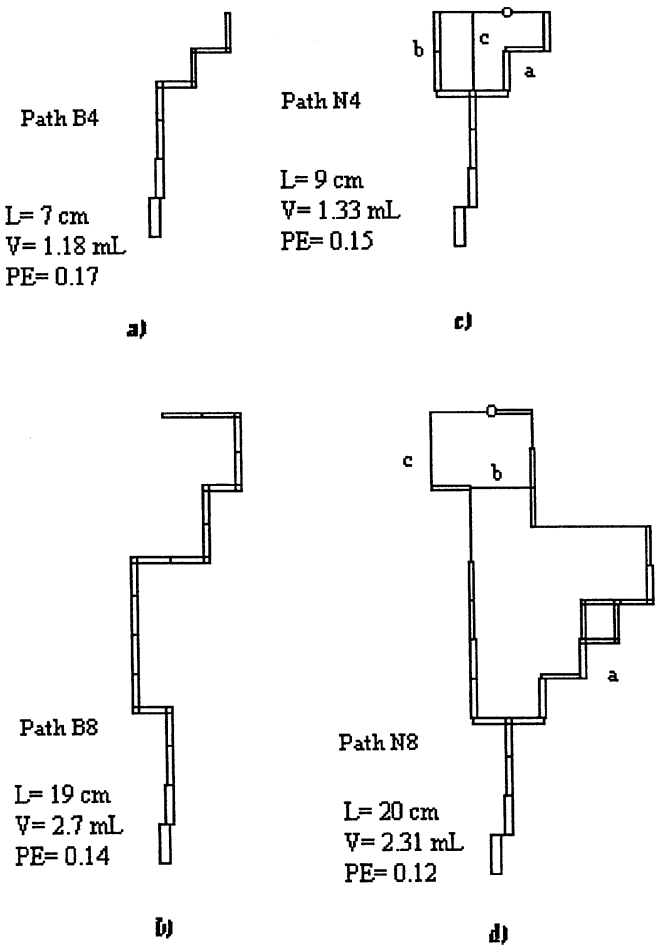

Figure 4. Diagram of selected flowpaths with the length (L) and volume (V) of each selected flowpath shown. The flowpaths are a) path 4 in the branchwork model; b) path 8 in the branchwork model; c) paths 4 a, b, & c in the network model; d) paths 8 a, b, & c in the network model. The length and volume refer to the pathway a in the network model.

EXPERIMENTAL SETUP

Distilled water was delivered to the top of the model through a recharge system that consisted of 256 pipette tips fed by a bifurcating system of tubes leading from a peristaltic pump (Fig. 5). The average rate of recharge was 2.2 ±0.6 mL/s. A syringe pump was used to inject a 1-M NaCl tracer onto the model at specified locations (Fig. 2) at 6.5 mL/min. A pulse input (9-s duration that resulted in the addition of 1 mL of solu-

Table 3. Average results from the tracer transport experiments using the network model. Each result is the average of N independent experiments.

Model	Lag (s)	Peak (s)	Mean (s)	DL (cm)	Pathlength (cm)	Pe	Re	Fr	Delta (mm)	N	Recovery (%)
location 1	5	12	40	3.0	8	8.7	61.3	0.004	0.20	9	14
location 2	3	10	27	2.3	8	16.0	85.0	0.006	0.17	8	22
location 3	4	12	28	1.2	7	13.0	68.7	0.005	0.17	9	28
location 4	3	12	23	0.9	9	20.3	92.0	0.009	0.15	9	24
location 5	3	12	24	1.1	8	15.0	83.7	0.008	0.15	10	29
location 6	2	27	50	2.5	19	14.7	85.0	0.009	0.19	6	12
location 7	7	27	51	2.8	16	11.0	82.0	0.007	0.20	4	18
location 8	5	21	53	6.2	20	8.0	88.0	0.008	0.19	6	31
location 9	7	19	51	17.0	17	11.3	96.0	0.004	0.18	7	40
location 10	5	15	38	4.4	21	11.7	107.7	0.014	0.16	3	40

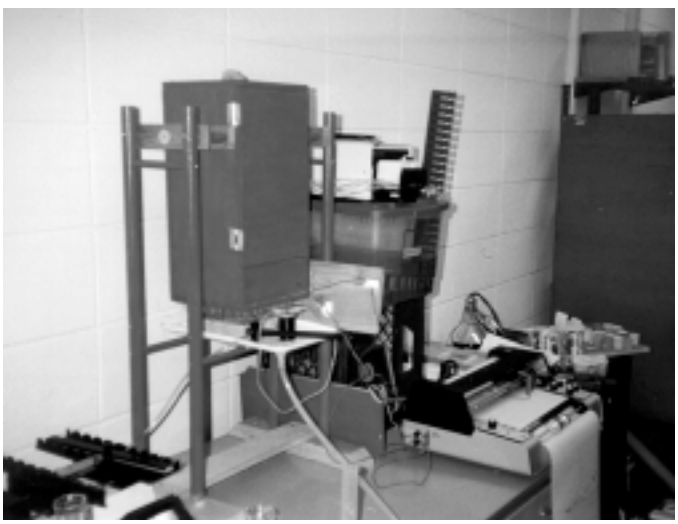

Figure 5. Photograph of the experimental apparatus showing the recharge water delivery system and the syringe pump used to introduce the tracer.

tion to the model) was used. The discharge from the model passed through a conductivity cell. The voltage across the conductivity cell was recorded with a strip-chart recorder and the data were digitized. Each conductivity cell was calibrated before and after each set of experiments to provide a conversion from voltage to concentration of tracer. The hydraulic gradient was 0.16 cm per 14.4 cm (1.1%) and was controlled by inserting shims beneath the upgradient end of the model.

EXPERIMENTS

Multiple replicate experiments were performed for each of ten matching input locations on the two models. The five input locations were equally spaced along an arc 3.3 cm from the spring. Another five input locations were equally spaced along an arc 6.8 cm from the spring. The input locations were independent of sinkhole locations, therefore the tracer was not injected directly into a sinkhole. However, at all input locations it was possible to determine based on sinkhole size or proximity to a sinkhole which sinkhole the tracer entered. As a result, the path that the tracer followed from an input location to the spring was determined and the path length was noted.

Breakthrough curves were plotted against time. For each of the experiments, the time to peak tracer concentration, the mean tracer transit time, the standard devation of the mean tracer transit time, longitudinal dispersivity, Peclet number, Reynolds number, Froude number, diffusion layer thickness, and percent tracer recovery were calculated using QTRACER (Field 1999). The values of the parameters were averaged for the replicate experiments.

RESULTS

For the tracer transport experiments using the branchwork model, the replicate breakthrough curves (concentration against time) exhibited a reasonable agreement for the injection location that was proximal to the spring and considerable variation for the injection location that was distal from the spring (Fig. 6; Table 2). The times to peak tracer concentration ranged from 10-18 sec. The mean tracer transit times ranged from 12-44 sec. The longitudinal dispersivity varied between 1.0 and 17 cm and represented 12.5-81% of the respective pathlength. The Reynolds and Froude were all within the laminar (<500) and subcritical (<1) flow region. The Peclet numbers (>6) indicated that advection dominated the transport processes. The diffusion layer thickness varied between 0.11 and 0.18 mm and represented 4-8% of the diameter of a class-five conduit.

For the tracer transport experiments using the network model, the replicate breakthrough curves (concentration against time) exhibited a reasonable agreement (Fig. 7; Table 3). The times to peak tracer concentration ranged from 11-26 seconds. The mean tracer transit times ranged from 23-55 seconds. The longitudinal dispersivity varied between 0.9 and 17 cm and represented 10-100% of the respective pathlengths. The Reynolds and Froude were all within the laminar (<500)

Figure 6.

Replicate breakthrough curves for the branchwork model using injection location 4 and injection location 8.

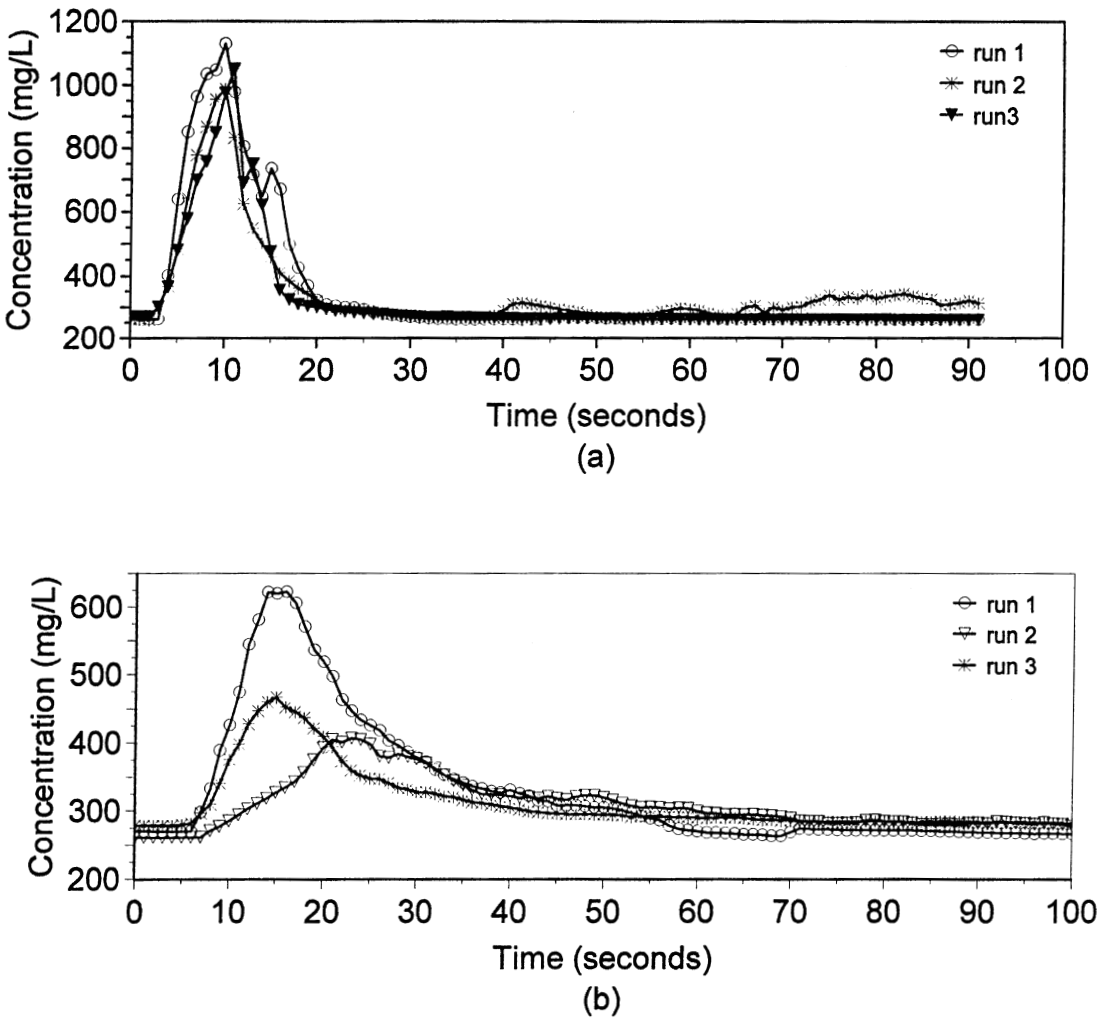

and subcritical (<1) flow regimes. The Peclet numbers (all >8) indicate that advection dominated the transport processes. The diffusion layer thickness varied between 0.15 and 0.20 mm and represented 6-8% of the diameter of a class-five conduit.

DISCUSSION

Our objectives were to develop laboratory-scale models of karstic aquifers, to conduct tracer transport experiments, to clearly document problems encountered, and most importantly, to provide data that could be used in calibrating numerical models. We have constructed scale models of karstic aquifers in which we controlled the length of the flow paths, the gradient, the recharge rate, the size of the conduits, and the geomorphic pattern of conduit layout.

We have calculated the Reynolds number and the Froude number for each and every experiment and have determined that the experiments were conducted under laminar, subcritical flow conditions. These conditions (laminar and subcritical flow) might be expected in karstic aquifers that have a low groundwater velocity, such as the Salem Plateau or the Floridan aquifer at locations away from the discharge points, the springs. These experiments are not applicable to karstic basins in which the water table intersects conduits, such as the Springfield Plateau. The models of karstic aquifers created in this study provided a means to conduct tracer transport experiments and generate data that are sufficient for validation of numerical models.

There are potential problems that require description and discussion. These are the potential for density-driven flow, the rate of recharge relative to the surface area of the model and the ratio of the diameter of the largest conduit to the surface area. Due to the difference in density of the recharging water (ρ = 1.00) and the tracer solution (ρ = 1.04), density-driven flow could have occurred in the models. Tracer transport experiments were also conducted using at 0.1 M (ρ =1.003) and 1.0 M NaCl to determine density effects (same injection rate, same injection location). Results (Florea 1998) were virtually identical (other than amplitude), thus effects from density-driven flow appear to be minimal. Another problem was the very high rate of recharge (2.2 mL/s over 100-cm² or 80 cm/hr) that was used. Although the rate of recharge was very high, it was reproducible (Tables 2 & 3). Finally, the volume of the conduits relative to the volume of the model (the porosity) was

Figure 7.

Replicate breakthrough curves for the network model using injection location 4 and injection location 8.

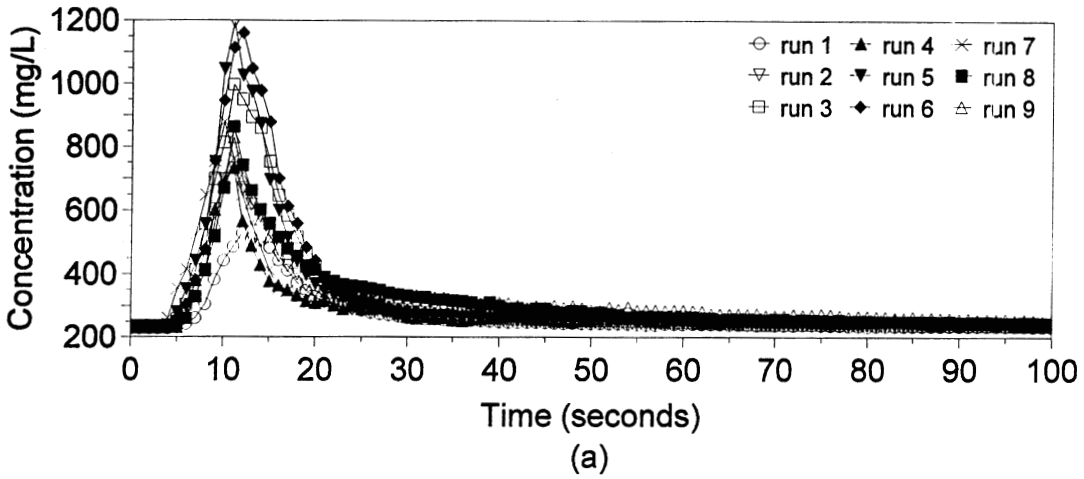

(a)

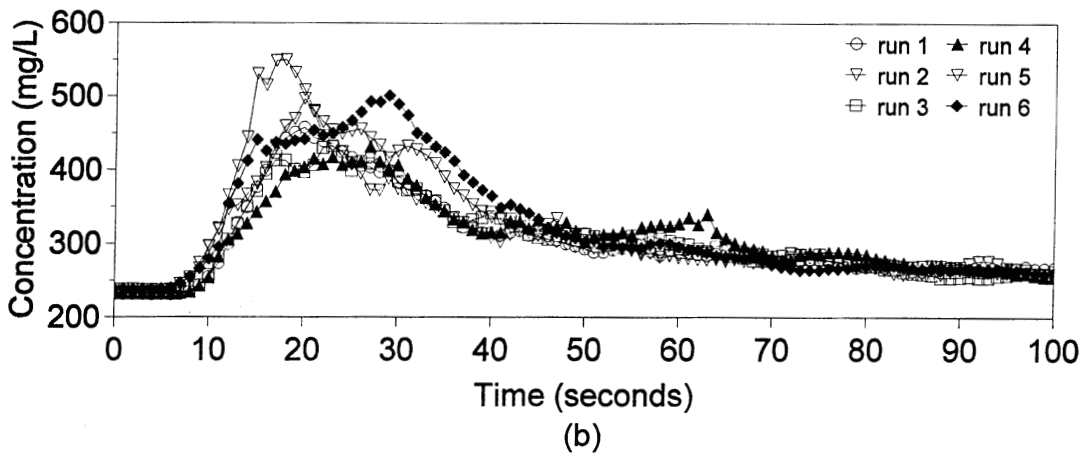

(b)

2.6% and 2.0% for the network and branchwork models, respectively. The porosity of the models was lower than the 12% porosity of Burlington Limestone (Hoag 1957), which we had chosen as typical cavernous limestone.

ACKNOWLEDGEMENTS

We acknowledge Bede Clark in the Department of Fine Arts at the University of Missouri-Columbia for use of his facilities and for aiding us in the creation of clay models. We thank Bill Annabelle and an anonymous reviewer for their helpful comments. We thank the University of Missouri Research Board (RB97-137C) for financial assistance. Acknowledgment is made to the Donors of The Petroleum Research Fund, administered by the American Chemical Society, for the partial support of this research.

REFERENCES

Anderson, M.P. & Woessner, W.W., 1992, *Applied Groundwater Modeling: Simulation of Flow and Advective Transport*: London, Academic Press, 381 p.

Annabelle, W.K. & Sudicky, E.A., 1999, On predicting contaminant transport in carbonate terrains: Behavior and prediction, *in* Palmer, A.N., Palmer, M.V., & Sasowsky, I.D., ed., *Karst Modeling*. Karst Waters Institute Special Publication 5, p. 133-145.

Bergstrom, D.E., 1997, The phylogeny and historical biogeography of Missouri's *Amblyopsis rosea* (Ozark cavefish) and *Typhlichthys subterraneus* (Southern cavefish) [MS thesis]: University of Missouri - Columbia, 63 p.

Curl, R.L., 1986, Fractal dimensions and geometries of caves: *Mathematical Geology*, v. 18, no. 8, p. 765-783.

Ewers, R.O., 1972, A model for the development of broad scale networks of subsurface drainage routes along bedding planes [MS thesis]: University of Cincinnati, 84 p.

Field, M.S., 1999, The QTRACER program for tracer-breakthrough curve analysis for karst and fractured-rock aquifers. U.S. Environmental Protection Agency, 600, R-98, 156 a, p. 137.

Florea, L.J., 1998, Bench-scale karst models [MS thesis]: University of Missouri - Columbia, 264 p.

Glew, J.R., 1977, Simulation of rillenkarren, *in Proceedings of the 7th International Congress of Speleological Congress*, Sheffield, UK, p. 218-219.

Hoag, W.M., 1957, Porosity and permeability of various paleozoic sediments in Missouri [MS thesis]: University of Missouri - Columbia, 72 p.

Ibaraki, M. & Sudicky, E.A., 1995a, Colloid-facilitated contaminant transport in discretely fractured porous media, 1, Numerical formulation and sensitivity analysis: *Water Resources Research*, v. 31, p. 2945-2960.

Ibaraki, M. & Sudicky, E.A., 1995b, Colloid-facilitated contaminant transport in discretely fractured porous media, 1, Fracture network examples: *Water Resources Research*, v. 31, p. 2961-2970.

Jeannin, P.Y., Hauns, M., & Atteia, O., 1999, Modeling breakthrough curves of tracing experiments in a karst environment, *in* Palmer, A. N., Palmer, M.V., & Sasowsky, I.D., ed., *Karst Modeling*. Karst Waters Institute Special Publication 5, p. 173.

Mohrlok, U. & Sauter, M., 1997, Modelling groundwater flow in a karst terrane using discrete and double-continuum approaches; importance of spatial and temporal distribution of recharge, *in Proceedings of the 12th International Speleological Congress*, p. 167-170.

Mohrlok, U. & Teutsch, G., 1997, Double continuum porous equivalent (DCPE) versus discrete modelling in karst terranes, *in Proceedings of the International Symposium and Field Seminar on Karst*, p. 319-326.

Padilla A. & Pado-Bosch, A., 1995, Study of hydrographs of karstic aquifers by correlation and cross-spectral analysis: *Journal of Hydrology*, v. 168, p. 73-89.

Palmer, A.N., 1991, The origin and morphology of limestone caves: *Geological Society of America Bulletin*, v. 103, p. 1-21.

Palmer, A N., 1999, Scale Models, *in* Palmer, A. N., Palmer, M.V., & Sasowsky, I.D., ed., *Karst Modeling.* Karst Waters Institute Special Publication 5, p. 176.

Peterson E.W. & Wicks, C.M., 2000, Modeling groundwater through branchwork conduit systems using the Storm Water Management Model (SWMM): *EOS Transactions of the American Geophysical Union*, v. 81, no. 48, p. 529.

Quinn, J. & Tomasko, D., 2000, A numerical approach to simulating mixed flow in karst aquifers, *in* Sasowsky, I.D. & Wicks, C.M., ed., *Groundwater flow and contaminant transport in carbonate aquifers*: Rotterdam, Balkema, p. 147-156.

Saiers, J. E. & Hornberger, G.M., 1994, First and second-order kinetic approaches for modeling the transport of colloidal particles in porous media: *Water Resources Research*, v. 30, p. 2499-2506.

Saiers, J.E., Hornberger, G.M., & Harvey, C., 1994, Colloidal silica transport through saturated, heterogeneous porous media: *Journal of Hydrology*, v. 163, p. 271-288.

Silliman, S.E., Konikow, L.F., & Voss, C.I., 1987, Laboratory investigation of longitudinal dispersion in anisotropic porous media: *Water Resources Research*, v. 23, p. 2145-2151.

Toran, L., Palumbo, A.V., 1992, Colloidal transport through fractured and unfractured laboratory sand columns: *Journal of Contaminant Hydrology*, v. 9, p. 289-303.

Troester, J.W. & White, E.L., & White, W.B., 1984, A comparison of sinkhole depth frequency distribution in temperate and tropical karst regions, *in* Beck, B. F., ed., *Sinkholes: Their geology, engineering, and environmental impact*: Rotterdam, Balkema, p. 65-73.

White, W.B., Culver, D.C., Herman, J.S., Kane, T.C., & Mylroie, J.E., 1995, Karst Lands: *American Scientist*, v. 83, p. 450-459.